Benefits of Artificially Generated Gravity Gradients for Interferometric Gravitational-Wave Detectors

L. Matone[1], P. Raffai[2], S. Márka[1], R. Grossman[1], P. Kalmus[1], Z. Márka[1], J. Rollins[1], V. Sannibale[3]

[1] Columbia University, Department of Physics, New York, NY 10027, USA
[2] Eötvös University, Institute of Physics, 1117 Budapest, Hungary
[3] California Institute of Technology, LIGO Laboratory, Pasadena, CA 91125, USA

Abstract. We present an approach to experimentally evaluate gravity gradient noise, a potentially limiting noise source in advanced interferometric gravitational wave (GW) detectors. In addition, the method can be used to provide sub-percent calibration in phase and amplitude of modern interferometric GW detectors. Knowledge of calibration to such certainties shall enhance the scientific output of the instruments in case of an eventual detection of GWs. The method relies on a rotating symmetrical two-body mass, a Dynamic gravity Field Generator (DFG). The placement of the DFG in the proximity of one of the interferometer's suspended test masses generates a change in the local gravitational field detectable with current interferometric GW detectors.

1. Introduction

Dynamic gravity fields generated by rotating masses have been used previously in several experimental tests; however, their exploitation in conjunction with interferometric gravitational detectors has not been addressed until now. Forward and Miller [1] in 1967 developed a gravity field generator that allowed them to calibrate an orbiter sensor capable of measuring the lunar mass distribution. A similar technique was used by Weber *et al.* [2, 3] to calibrate a GW bar detector, where a volume of matter was acoustically stressed at 1660 Hz and the resulting noise excess in the detector was found to be consistent with theory. At the University of Tokyo, in the 1980s, a series of experiments were conducted to test the law of gravitation up to a distance of 10 m [4, 5, 6, 7, 8]. In these studies, the coupling between the dynamic field, generated by a rotating mass, and the quadrupole moment of a mechanical oscillator antenna was measured confirming the gravitational law within experimental uncertainties [7, 8]. In the 1990s, the gravitational wave group at the University of Rome developed and carried out experiments [9, 10] on the cryogenic GW bar detector, EXPLORER, at CERN. A device, with quadrupole moment of $\mathcal{M}_2 = 6.65 \times 10^{-2}$ kg m^2 and rotating in the frequency range of $450 - 470$ Hz, was developed to calibrate the antenna and was also used to confirm existing upper limits to Yukawa-like gravitational potential violations at laboratory scale.

The increased sensitivity and bandwidth of modern interferometric gravitational wave detectors warrants a new investigation into and opens exciting new possibilities for application of advanced gravity field generators in GW research. Presently interferometric gravitational wave detectors are reaching their design sensitivity enabling us to probe for gravitational radiation from sources well beyond the Local Group of galaxies. The response of these detectors to GW radiation is usually evaluated by direct injection of possible waveforms with known amplitude via magnetic actuators, also used for active control of the test masses' (essentially the interferometer mirrors) displacement. In addition, displacement in the test mass position can be induced by local gravity fields produced by a Dynamic gravity Field Generator (DFG). A DFG is essentially a symmetric rotating object with a significant quadrupole moment. When it is placed in the proximity of one of the interferometer mirrors, the induced change due to the device's quadrupole moment can be measured by the GW detectors such as the Laser Interferometer Gravitational Wave Observatory (LIGO) [11, 12], the VIRGO experiment [13], the 300 m Laser Interferometer Gravitational Wave Antenna (TAMA300) [14] and the GEO600 interferometer [15]. Future detectors, such as Advanced LIGO (AdLIGO) [16], offer higher sensitivity.

Several authors (see for example [17, 18, 19]) pointed out that gravity gradient (or Newtonian) noise, generated by density fluctuations in the Earth and the atmosphere, can be a potentially limiting noise source in advanced interferometric GW detectors. Motion of massive bodies (e.g. due to human activity) in the vicinity of the interferometer test masses also alters the local gravitational field, mainly at low frequencies [20, 21, 17]. Gravity gradient noise manifests itself as an induced motion of the interferometer mirrors due to the fluctuation of the local gravity field. The DFGs described here can be used to modulate the local gravitational field around the test mass (TM) at a precise frequency and phase on a well-controlled manner and thereby directly validate/evaluate the expected noise generation and coupling mechanisms to complex structures.

In addition, DFGs have the potential to provide sub-percent amplitude and phase calibration of interferometric GW detectors. In the case of LIGO, currently there are two calibration methods in use. The first one uses the interferometer TM's coil-magnet actuator to calibrate the gravitational wave channel (see for example [22] and [23]) while the second method uses the radiation pressure exerted on the TM by an independent laser source (see for example [24], [25], [26] and recently [27]). A DFG provides an alternative and independent sub-percent calibration, significantly improving the current accuracy of several percents (see e.g. [28]).

In this work we describe a hypothetical two-body DFG coupled to an ideal interferometric gravitational wave detector. The induced displacement on the suspended TM is dominated by the quadrupole moment of the DFG mass distribution in the case of a symmetric device. Any undesired system asymmetry will contribute to the dipole moment and can be measured and accounted for directly. We asses the application of such devices for the calibration of interferometric GW detectors as well their possible usage in gravity gradient noise studies that will eventually limit the performance of long baseline detectors at low frequencies.

Additionally, two DFGs in a null experiment setup can be used to explore violations to Newton's $1/r^2$ law well beyond the current limits. We investigated this possibility in detail for LIGO, Advanced LIGO and Virgo detectors via numerical simulations. This is the subject of a separate publication. [29]

2. Newtonian field dynamics from a two-mass DFG

In analytical derivations, throughout this paper we will treat the suspended interferometer TM and the masses of the two-body DFG as point masses for simplicity. First we calculate the acceleration, along the laser beam axis, the mass is subjected to from a DFG configuration shown in fig.(1). Masses m_1 and m_2 are separated by a distance r_1 and r_2, respectively, from the center of rotation and are rotating at a frequency of $f_0 = \omega_0/(2\pi)$. The center of mass of mirror M and the DFG's center of rotation are separated by a distance d, where $d > r_{1,2}$.

Assuming that the distance between the DFG's i-th mass and the mirror is h_i, the Newtonian potential at the mirror's center of mass is

$$V^\mathrm{c} = \sum_{i=1}^{2} V_\mathrm{i}^\mathrm{c} = -GM \sum_{i=1}^{2} \frac{m_\mathrm{i}}{h_\mathrm{i}}. \tag{1}$$

Introducing the variables $R_1 = r_1/d$, and $R_2 = -r_2/d$, h_i, being a function of time can

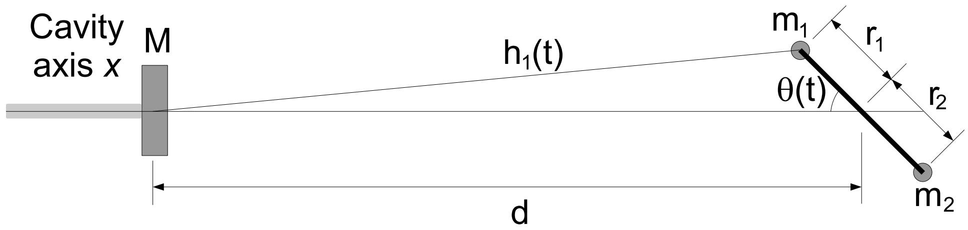

Figure 1. Schematic of an ideal symmetric two-mass DFG. The system consists of two masses, m_1 and m_2, separated by a distance of r_1 and r_2 from the center of rotation. The center of rotation is placed a distance d away from the mirror's center of mass. The system rotates at a frequency of $f_0 = \omega_0/(2\pi)$ where $\theta(t) = \omega_0 t$. The x axis denotes the interferometer's optical axis and only accelerations along this axis are considered.

be written as

$$h_{\mathrm{i}}(t) = d\,\sqrt{1 + R_{\mathrm{i}}^2 - 2R_{\mathrm{i}}\cos\theta(t)} \tag{2}$$

where $\theta(t) = \omega_0 t$ (see fig.(1)). The magnitude of the TM's induced acceleration along the laser beam axis is

$$a^{\mathrm{c}} = \frac{1}{M}\left|\frac{\partial V^{\mathrm{c}}}{\partial d}\right| = \frac{G}{d^2}\sum_{i=1}^{2} m_{\mathrm{i}} B_{\mathrm{i}}(R_{\mathrm{i}},\theta). \tag{3}$$

Here $B_{\mathrm{i}}(R_{\mathrm{i}},\theta)$ is a geometrical factor

$$B_{\mathrm{i}}(R_{\mathrm{i}},\theta) = \frac{1 - R_{\mathrm{i}}\cos\theta}{(1 - 2R_{\mathrm{i}}\cos\theta + R_{\mathrm{i}}^2)^{3/2}}. \tag{4}$$

For the case of a much smaller lever arm r_{i} than the distance d ($R_{\mathrm{i}} \ll 1$) we can expand V^{c} thereby expressing the induced acceleration a^{c} in terms of the n-th multipole moment $\mathcal{M}_{\mathrm{n}}$ of the DFG's mass distribution

$$a^{\mathrm{c}} = \frac{G}{d^2}\sum_{n=0}^{\infty} \frac{n+1}{d^n}\cdot\mathcal{M}_{\mathrm{n}}\cdot P_{\mathrm{n}}(\cos\theta) \tag{5}$$

where

$$\mathcal{M}_{\mathrm{n}} = m_1 r_1^n + (-1)^n m_2 r_2^n \tag{6}$$

and $P_{\mathrm{n}}(\cos\theta)$ is the Legendre polynomial of n-th order.

We remark that the DFG's dipole moment, as well as the higher-order odd moments, contribute only to the odd harmonic terms, whereas the quadrupole moment and the higher-order even terms, contribute only to the even harmonic terms. In the case of an ideally symmetric DFG, all odd moments vanish and the induced displacement is dominated by the quadrupole moment $\mathcal{M}_2$ at twice the rotation frequency.

2.1. Induced Displacement from the Newtonian Potential

The suspended TM can be considered as a free body for frequencies well above the eigenfrequencies of the suspension which typically lie around 1 Hz [30]. Neglecting the time-independent term, double integrating eq.(5) with respect to time and considering only the dominant terms in the first few harmonics, the TM's displacement along the laser beam axis, x, can be written as

$$x(t) \simeq \frac{G}{(d\,\omega_0)^2} \times \left[2 \cdot \frac{\mathcal{M}_1}{d} \cdot \cos\omega_0 t + \frac{9}{16} \cdot \frac{\mathcal{M}_2}{d^2} \cdot \cos 2\omega_0 t + \frac{5}{18} \cdot \frac{\mathcal{M}_3}{d^3} \cdot \cos 3\omega_0 t\right] \tag{7}$$

In the case of a symmetric two-mass DFG, the dipole and the octopole contribution vanishes and the quadrupole moment $\mathcal{M}_2$ dominates. For initial LIGO throughout the paper we will consider the case of $m_1 = m_2 = 1.5$ kg, $r_1 = r_2 = 0.25$ m (equivalent to a quadrupole moment of $\mathcal{M}_2 = 0.1875$ kg m^2), with a rotation frequency of $f_0 = \omega_0/(2\pi) = 51$ Hz and a distance of $d = 2.5$ m. The resulting RMS displacement change $x_{\rm rms}$ at twice the rotation frequency is 1.24×10^{-18} m and scales according to

$$x_{\rm rms} \simeq 1.24 \times 10^{-18}\ \mathrm{m} \times \left(\frac{\mathcal{M}_2}{0.1875\ \mathrm{kg\ m^2}}\right) \times \left(\frac{51\ \mathrm{Hz}}{f_0}\right)^2 \times \left(\frac{2.5\ \mathrm{m}}{d}\right)^4 \tag{8}$$

Fig.(2) shows the design sensitivities for initial LIGO, AdLIGO and VIRGO also including LIGO's nominal displacement sensitivity for the beginning of the fifth science run [31] (S5). The LIGO detectors' displacement sensitivity at 102 Hz is $\sim 2 \times 10^{-19}$ m/$\sqrt{\mathrm{Hz}}$ (see gray curve in fig.(2)).

The signal-to-noise ratio (SNR), defined as the ratio of the RMS signal to the displacement noise spectrum density integrated for a time T, gives a measure of how much a given stimulus is above background. For the above mentioned device, in the case of LIGO during S5 at 102 Hz (that is twice the above mentioned rotation frequency), and for an integration time of 1 s, we obtain an SNR of 6. In general terms, for an arbitrary noise floor $\tilde{n}$, and integration time T, the SNR scales as

$$SNR \simeq 6 \times \left(\frac{2 \times 10^{-19}\ \mathrm{m}/\sqrt{\mathrm{Hz}}}{\tilde{n}}\right) \times \times \left(\frac{T}{1\ \mathrm{s}}\right)^{1/2} \times \left(\frac{x_{\rm rms}}{1.24 \times 10^{-18}\ \mathrm{m}}\right) \tag{9}$$

where $x_{\rm rms}$ is shown in eq.(8). At the present sensitivity level of LIGO it is possible to sense such a dynamically changing gravity field from the DFG in question using a relatively small integration time.

Fig.(3) shows the SNR for different detectors as a function of twice the rotational frequency with an integration time of half an hour. Using once again the example cited above (DFG of quadrupole moment $\mathcal{M}_2 = 0.1875$ kg m^2), the top portion of the figure shows, that for rotational frequencies ranging between 10 Hz and 500 Hz, a distance of 2.5 m can be used for the initial LIGO detectors.

The center part of fig.(3) shows the SNR for the VIRGO detector. Due to the detector's sensitivity at low frequencies, low rotational frequencies, as low as ~ 10 Hz,

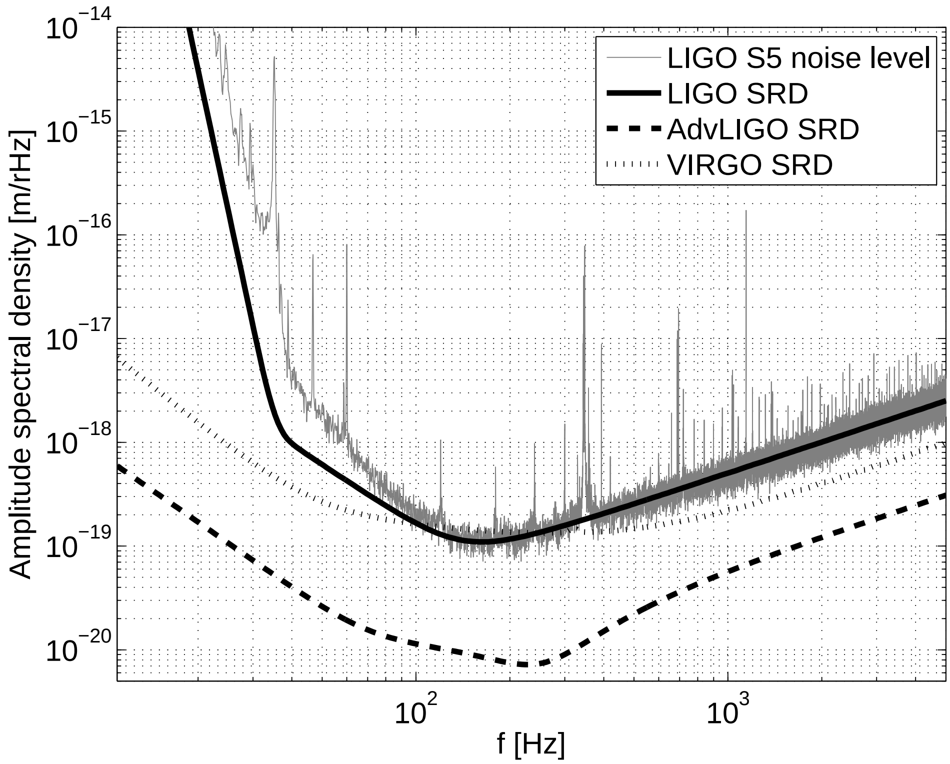

Figure 2. The nominal displacement sensitivity of LIGO (gray trace) at the beginning of the fifth science run (S5) together with its design curve (black); the design sensitivity (SRD) for Advanced LIGO (dashed) and the European VIRGO detector (dotted) are also shown.

could be used. The bottom portion of fig.(3) shows the response from the Advanced LIGO interferometer.

2.2. A hypothetical DFG design

In fig.(4) we show a hypothetical DFG design based on the parameters discussed in this section. It consists of an Aircraft Grade (6Al/6V/2Sn) Titanium disc 60 cm in diameter and 10 cm in height. The disc has two cylindrical slots, 50 cm apart, which can hold different materials. The choice of materials was motivated by the desire to maximize density difference and strength while still keeping the material cost within the bounds of reason. We use Tungsten cylinders 3.6 cm in diameter, corresponding to an effective mass difference of 1.5 kg, as an example in the following sections. Practical details, such as the expansion and stress factors of the DFG under prolonged operating conditions must be modeled and simulated by finite element analysis methods, then subsequently measured and taken into account. These studies are beyond the scope of this paper.

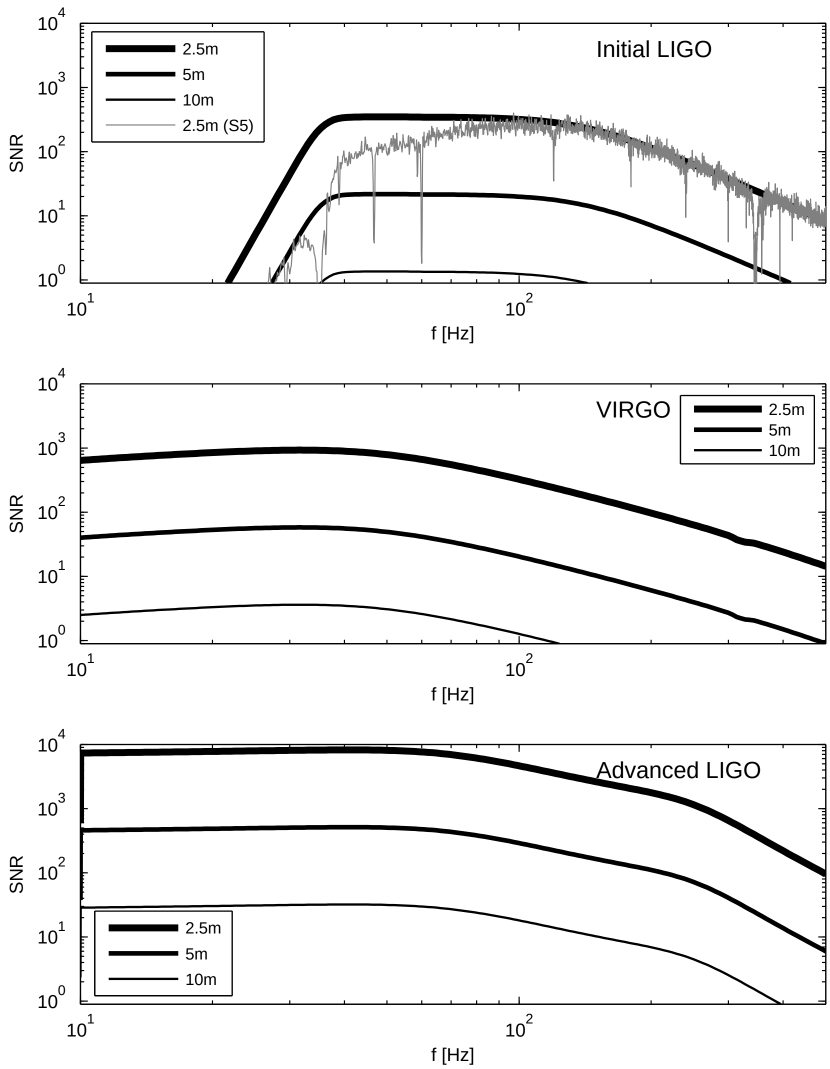

Figure 3. The Signal-to-Noise Ratio due to a DFG of quadrupole moment $\mathcal{M}_2 = 0.1875$ kg m^2 and 1/2 hour of integration time. Top: initial LIGO with the DFG positioned 2.5, 5 and 10m away from the TM; Middle: VIRGO for positions of 2.5, 5, and 10m; Bottom: Advanced LIGO with distances to the TM of 2.5, 5 and 10m.

2.3. Gravity Gradient Noise Studies with DFGs

A DFG in the proximity of the test mass of the interferometer can be used to experimentally investigate and model the coupling between the varying gravity field and the complex suspension system of the test mass in many fundamental configurations. The artificial gravity gradient field generated by a DFG not only couples to the test mass but also into all stages of the multistage suspension system and gives rise to possible second order effects. By varying the placement and rotation frequency of the

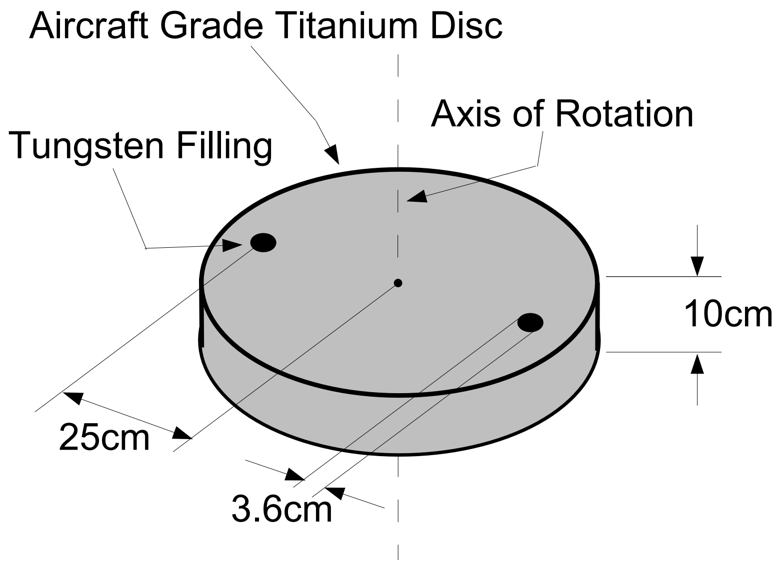

Figure 4. Sketch of a hypothetical DFG. The DFG consists of an Aircraft Grade (6Al/6V/2Sn) Titanium disc 60 cm in diameter and 10 cm in height. It holds two Tungsten cylinders at 25 cm from the rotation axis. The diameter of the Tungsten cylinders is 3.6 cm.

DFG, this artificial gravity field can simulate conceivable gravity gradient noise sources specific to the local environment of the interferometric detector in question. With a DFG, the dependence of the TM's displacement on the orientation of the gravity gradient noise source can be mapped: the DFG can be installed at different distances from the TM in the axis of the laser beam as well as placed off-axis and out of the plane of the interferometer. This is especially important since gravity gradient noise couples to the system from each direction on different ways thus potentially introduces problems into the detection chain via hard to track second order effects and possible nonlinear couplings. Additional advantage of artificially generated dynamic gravity gradients is that the frequency dependence of the interferometer's response to Newtonian noise sources could be mapped out in detail, which is especially important for the low frequency region. The results might eventually be used in generating approaches for mitigating the effect of local gravity gradients in future detectors at low frequencies besides providing accurate information about the nature of this noise source.

2.4. Calibration of an Interferometric GW Detector using a DFG

In this section we address the level of precision we must achieve when using the DFG as a calibration tool. While the present calibration accuracy of 2-10% in amplitude and phase [28] (depending on frequency range) might seem adequate for upper limit and event rate studies, it will be important to know the calibration of the detector to a higher accuracy when the collaborations enter the "detection era". Subpercent amplitude calibration becomes important when signals with sufficiently large signal to noise ratios are observed. In the context of a detected signal via a global network of interferometric GW detectors, where the waveform is recoverable, phase calibration known to a higher precision shall be beneficial. Coherent network methods will perform better, pointing accuracy will increase, source distance information can be recovered and used with a higher accuracy. With an increase in calibration certainty the precision of waveform and polarization recovery is expected to improve, which in turn allows for better scientific output.

With the DFG method, the achievable calibration accuracy would be limited by the uncertainty in the gravitational constant, G, at the subpercent level. To estimate the calibration uncertainty we first consider the TM displacement $x_{\rm rms}$ induced by the DFG due to its quadrupole moment $\mathcal{M}_2$ is given in eq.(8). In statistical terms (assuming a large number of DFGs identical within practical tolerances), the relative uncertainties in the measurement of the gravitational constant $(\delta G/G)$, in the mass $(\delta m/m)$, arm length $(\delta r/r)$, rotation frequency $(\delta f_0/f_0)$ and distance from the TM center of mass $(\delta d/d)$ add in quadrature leading to a relative uncertainty on the induced displacement $(\delta x/x)$ and is approximately described by

$$\left(\frac{\delta x}{x}\right)^2 \simeq \left(\frac{\delta G}{G}\right)^2 + \left(\frac{\delta m}{m}\right)^2 + 4\left(\frac{\delta r}{r}\right)^2 + + 4\left(\frac{\delta f_0}{f_0}\right)^2 + 16\left(\frac{\delta d}{d}\right)^2 \tag{10}$$

Our goal is to achieve sub-percent precision in amplitude calibration, therefore we need to keep the relative uncertainties of every DFG parameter well below $\simeq 0.1\%$.

The currently accepted value of the gravitational constant, G, is $((6.6742 \pm 0.0010) \times 10^{-11} \mathrm{m}^3\mathrm{kg}^{-1}\mathrm{s}^{-2})$. This means, that there is a $\simeq 0.015\%$ contribution to the relative uncertainty on the induced displacement just by taking into consideration the precision of previous G measurements. G contributes as the leading term in limiting the precision of amplitude calibration if the uncertainties related to manufacturing and/or measurement of the other parameters contributing to each of the other four terms in equation (10) is below 0.015%. Thus we require

$$\begin{aligned} \frac{\delta m}{m} &\leq 1.5 \times 10^{-4} \\ \frac{\delta r}{r} &\leq 7.5 \times 10^{-5} \\ \frac{\delta f_0}{f_0} &\leq 7.5 \times 10^{-5} \\ \frac{\delta d}{d} &\leq 3.75 \times 10^{-5} \end{aligned} \tag{11}$$

These levels of uncertainties adding up in quadrature yield 0.035% uncertainty in $(\delta x/x)$, more than adequate for a sub-percent amplitude calibration.

Considering the DFG described in sec.(2.1), with $m_1 = m_2 = 1.5$ kg, $r_1 = r_2 = 0.25$ m, rotation frequency of $f_0 = 51$ Hz and distance from the TM of $d = 2.5$ m, the required uncertainties in (11) translate to

$$\begin{aligned} \delta m &= 2.25 \times 10^{-4} kg \\ \delta r &= 1.9 \times 10^{-5} m \\ \delta f_0 &= 3.8 \times 10^{-3} Hz \\ \delta d &= 9.4 \times 10^{-5} m \end{aligned} \tag{12}$$

Most precision off-the-shelf balances can be used to measure the DFG masses, while the ultimate precision of mass determination, δm, is ~ 50 μg [32] with a state of the art mass comparator. Uncertainties on δr are determined by machining precision and can be kept within ~ 1 μm [33].

The uncertainty in the rotational frequency f_0 can be addressed by using a precision optical encoder to provide pulses which can be used to phase lock the absolute angular position of the DFG to an atomic clock or GPS. In this case, the uncertainty is limited by the encoder itself or the servo system. For a rotation period of $1/f_0 = 20$ ms and an off-the-shelf 16-bit optical encoder providing a square pulse train at 3.2 MHz ($\simeq 300$ ns/pulse), the relative position of the square wave rising edge with respect to the atomic clock signal can be determined for better than $\delta t \simeq 10$ ns. This allows for a high precision of $\delta f_0/f_0 \sim 10^{-6}$.

Distance d could change somewhat over time when a DFG is used as a calibration device. The thermal variations in the TM and DFG housings are kept within fractions of a degree and should not play a significant role. The tidal-compensation system, a servo-mechanism acting on the position of the TM to compensate for earth-moon and earth-sun tidal effects, displaces the TM locally with peak to peak excursions of the order of ~ 300 μm (see [34] and [35]). This kind of excursion can be taken into account during the calibration.

Distance d can be directly measured via laser based range finding (i.e. Light Detection and Ranging, LIDAR) technologies, which can provide better than $\delta d \simeq 1$ μm uncertainty in lab environments [36].

When direct distance measurement between the TM and the DFG is not possible, an alternative method for finding d can be adopted. The $2\omega_0$ component can be measured as a function of d by varying the DFG's position by a well known amount and using a χ^2 minimization procedure to estimate the effective distance d. For simplicity, let the distance vary linearly

$$d(t) = d_0 + v\ t \tag{13}$$

where v is the DFG's pivot velocity along the beam axis. Following eq.(8), the uncalibrated interferometer response R_{IFO} to the DFG's stimulus can be described as

$$R_{IFO} = \frac{K}{(d_0 + v\ t)^4} \tag{14}$$

where K and d_0 are free parameters. A linear sweep of the pivot's position would provide an estimate of d_0 while any residual would provide information on any $d(t)$ component that could potentially be significant. The uncertainty in d_0 will be statistical in nature and eventually will be limited to the systematic uncertainty of the other parameters, such as the dipole moment and the rotation frequency. In this case

$$\frac{\delta d}{d} \sim \frac{\delta r}{r} \sim 10^{-5} \tag{15}$$

There are also other uncertainties that need to be addressed for realistic measurements, most of them are second order in nature. For example, stress under operation conditions results in the deformation of the rotating DFG. The length change for a titanium 50 cm long 10 cm diameter rod holding two 1.5 kg masses at both ends is estimated to be at the order of 10 μm. For the proposed DFG design (4) this source of uncertainty should be significantly less and can be carefully modeled, measured and taken into account with a sub-μm accuracy.

An accurate alignment of the DFG is also necessary: the effective arm length $\tilde{r}$ is altered if the plane of rotation of the DFG is not aligned with the plane of the interferometer. Restricting this change to 19 μm (same as the uncertainty required for r) restrains the leveling of the DFG to 0.7°, which is achievable with commercial optical positioning methods.

The absolute phase of the rotating DFG can be measured by phase locking the DFG to an atomic clock or GPS. The phase uncertainty due to $\delta t/t$ is therefore based on $\delta f_0/f_0 \sim 10^{-6}$, therefore the precision of phase calibration for a perfectly oriented DFG can even be better than $\simeq 0.01\%$.

Placing the DFG out of line with the Fabry-Perot arm introduces other second-order error sources. First, it creates a distance $\tilde{d}$ which differs from d. Requiring their relative change $(\tilde{d} - d)/d$ to be of the order of 10^{-5} sets an alignment requirement to the cavity with an order of 1 cm. Additionally, a DFG not centered on the axis of the laser beam introduces an error in phase determination. In order to achieve 0.01% phase calibration this alignment requirement is constrained to 250 μm, which is still achievable with optical positioning.

The quoted accuracy of calibration for the LIGO detector for recent science runs [28] is at the 6-10% level and valid for a broad range of frequencies and for the entire length of the science run. The inherent accuracy of the calibration method itself is at the order of 1-2% [37]. Using DFG as calibration tool this can be pushed down to the subpercent level for amplitude and phase calibration.

To take full advantage of this proposed calibration method for interferometric GW detectors, we envision a DFG positioned at around 2-3 m from each end mirror of the two arms of the interferometer. The rotation frequencies can be chosen such that subpercent level calibration could be provided for the most sensitive region of the detector response. The employment of two separate DFGs, rotating at slightly different frequencies, would allow the calibration of the two interferometer arms separately in a spectrally similar region. Additionally, with longer integration times higher order harmonics become detectable. Thus the device can be used for calibration of interferometer response of frequency regions at points separated by the DFG's rotation frequency. From signals at the higher harmonics, information on the actual DFG parameters might also be deduced.

3. Mitigation of Spurious Couplings from the DFG's Motor

In interferometric GW detectors, using DFGs as a calibration tool means that the new device will be put in close proximity (e.g. 2.5 meters) of the test mass for a prolonged period of time, while the GW detector itself is in a continuous data taking mode. Thus, it is necessary that spurious coupling of the DFG to the suspended mirror be negligible, as detailed in this chapter. The only acceptable effect on the GW data should be the fine and easily filterable lines at the multiples of the rotational frequency of the DFG. Of most concern is the electro-magnetic coupling via the motor driving the system, the acoustic coupling via the local interferometer optical sensors and the seismic vibrations induced by an unbalanced DFG.

3.1. Electro-Magnetic Coupling

There are two ways the motor's electro-magnetic field could couple to the test mass. One coupling is the interaction of the motor's electro-magnetic (EM) field with the interferometer electronics residing next to the DFG. The other way is through the coupling of the DFG's EM field with the coil-magnet system needed to drive the TM in position.

With the proper Electromagnetic Interference (EMI) shielding in place and using DC permanent magnet servo motors the parasitic emission can be mitigated. The DFG could be equipped with a non-integer gear ratio to completely separate the EM harmonics from the Newtonian signal since the induced displacement appears at harmonics of the rotation frequency of the DFG and not of the motor.

It is also possible to completely eliminate the mechanical coupling via an Eddy Current Motor, which simplifies the DFG balancing and bearing design. Alternatively one can use an air motor which also eliminates the need for a gear-box mechanism.

3.2. Acoustic coupling

For the LIGO interferometers, acoustic signals near the detector could potentially couple directly to the gravitational wave channel. A possible coupling mechanism could consist of an acoustic stimulus exciting the beam position on an optical sensor. If the sensor in question is used to feedback on TM positions, the acoustic excitation finds its way into the detector. This effect is mitigated by installing the DFG in its own vacuum envelope.

3.3. Seismic coupling

One should also estimate the level of contamination into the GW datastream, due to the coupling of seismic disturbances through the ground, caused by the rotating device. This effect is the greatest at the rotation frequency and should be considerably smaller at the second and higher harmonics. For an ideally symmetric DFG, as described in earlier sections, the dipole moment vanishes and so does its contribution to the Newtonian field. Any asymmetry in the system creates a non-null dipole moment at the rotation frequency, introducing ground vibration. In this section we use a simple model to estimate this cross-coupling for the initial LIGO case.

For an asymmetric DFG, the device's center of rotation will be subjected to a sinusoidal force F' at the rotation frequency ω_0 whose RMS value along the beam axis can be written as

$$F'_{\rm rms} = \frac{1}{\sqrt{2}}\,\omega_0^2\,\mathcal{M}_1 \tag{16}$$

where $\mathcal{M}_1$ is the dipole moment of the DFG. The displacement $\delta x_{\rm react}$ of the reaction mass due to the asymmetry, to first order approximation, is

$$\delta x_{\rm react} = \frac{m\,r}{\sqrt{2}\,M_{\rm react}}\,(\epsilon_r + \epsilon_m) \tag{17}$$

where $\epsilon_r = \delta r/r$ and $\epsilon_m = \delta m/m$. The TM displacement can then be expressed as

$$\delta x_{\rm rms} = \delta x_{\rm react}\ \mathrm{R(f)} \tag{18}$$

where R(f) is the attenuation factor provided by LIGO's seismic isolation stage and suspension.

To estimate the motion of the cement slab beneath both the DFG and the TM we select achievable uncertainty requirements of (11). For a plausible reaction mass $M_{\rm react}$ of 100 tons (assuming a concrete slab $10m \times 10m \times 0.5m$) its mass displacement is

$$\delta x_{\rm react} = 6 \times 10^{-10}\mathrm{m} \tag{19}$$

LIGO's stack[38] reduces this displacement down by a factor of $\sim 10^6$ at 51 Hz while the suspension stage [30] brings it down by an another factor of $\sim (51\ \mathrm{Hz}/0.74\ \mathrm{Hz})^2 = 4500$. This results in a TM displacement of

$$\delta x_{\rm rms} = 1.3 \times 10^{-19} m \tag{20}$$

which is below the noise floor of LIGO and is only detectable with $SNR = 3$ after half an hour integration time.

The above estimated effect of seismic coupling can be further reduced by attaching the rotating DFG to a light slab with very small reaction mass $M_{\rm react}$. The seismic signal of a high-precision seismometer coupled to the slab, resulting from system asymmetries, can be substantially reduced by iterative adjustment of the balancing of the DFG. Attaching this balanced DFG to a heavy slab with higher $M_{\rm react}$ will reduce $\delta x_{\rm react}$ to be well below the ambient seismic field. The reduction factor is given by the ratio of the reaction mass of the light slab to the reaction mass of the heavy slab. This can lead to a TM RMS displacement even orders of magnitude smaller than as given in eq.(20).

4. Safety

Significant kinetic energy (i.e. tens of kJs) is stored in the DFG once it rotates and crucial safety considerations must be addressed. There are two major points of failure management to be concerned with. (a.) The vacuum chamber of the DFGs must be made strong enough to withstand the damage of an accidentally disintegrating disk. This is the standard solution for high speed gyroscopes. (b.) For added security, the gap between the inner wall of the vacuum chamber and the outer edge of the rotating disk must be kept relatively *small*. In the event of an incident where the DFG's material starts to yield or its angular acceleration is uncontrolled the disk will expand radially touching the sidewall and slowly stop, preempting a catastrophic failure. These conditions can be met using Finite Element Analysis (FEA) aided design, in-house destructive testing of sacrificial parts and relying only on X-ray rated base materials.

5. Conclusion

These initial feasibility studies of simple DFGs indicate that they are capable of dynamically changing the local gravitational field by an amount detectable by current interferometric gravitational wave detectors.

The DFGs can be designed, manufactured, tuned and characterized to be symmetric and safe enough to eliminate concerns about vibrations and spurious couplings, once positioned in the proximity of one of the suspended TMs.

The generated gravity gradient signal is proportional to the DFG's quadrupole moment with its signature appearing at twice the rotation frequency. At the present detector sensitivity level of LIGO, systematic uncertainties due to the DFGs can be well below the 0.1% level in amplitude with insignificant timing uncertainties. This apparatus provides a detector-independent calibration technique that can significantly surpass the achievable precision of other existing calibration methods.

The DFG also offers a unique and distinctive way to generate a differential arm length displacement for gravitational wave detectors. Apart from calibration objectives, it could also be used to validate the expected noise generation and coupling mechanism of Newtonian noise, possibly a limiting factor in advanced gravitational wave detectors.

There are many details that need attention when designing and manufacturing a practical device. Finite element analysis of the DFGs and subsequent experimental studies are necessary to completely understand the stresses the DFG is subjected to. The DFGs will be enclosed in a separate vacuum chamber. A prototype design and test will be necessary to balance the disk and test vibration control. Other mostly practical problems, such as safety, can also be solved as was shown in past applications/experiments that have used rapidly rotating instruments.

6. Acknowledgements

The authors are grateful for the support of the United States National Science Foundation under cooperative agreement PHY-04-57528 and Columbia University in the City of New York. We greatly appreciate the support of LIGO collaboration. We are indebted to many of our colleagues for frequent and fruitful discussion, and for the LIGO Scientific Collaboration Review. In particular we'd like to thank G.Giordano, R.Adhikari, V.Sandberg, M.Landry, P.Sutton, P.Shawhan, D. Sigg, R.DeSalvo, H.Yamamoto, Y. Aso and C.Matone for their valuable comments on the manuscript.

The authors gratefully acknowledge the support of the United States National Science Foundation for the construction and operation of the LIGO Laboratory and the Particle Physics and Astronomy Research Council of the United Kingdom, the Max-Planck-Society and the State of Niedersachsen/Germany for support of the construction and operation of the GEO600 detector. The authors also gratefully acknowledge the support of the research by these agencies and by the Australian Research Council, the Natural Sciences and Engineering Research Council of Canada, the Council of Scientific and Industrial Research of India, the Department of Science and Technology of India, the Spanish Ministerio de Educacion y Ciencia, The National Aeronautics and Space Administration, the John Simon Guggenheim Foundation, the Alexander von Humboldt Foundation, the Leverhulme Trust, the David and Lucile Packard Foundation, the Research Corporation, and the Alfred P. Sloan Foundation.

The LIGO Observatories were constructed by the California Institute of Technology and Massachusetts Institute of Technology with funding from the National Science Foundation under cooperative agreement PHY-9210038. The LIGO Laboratory operates under cooperative agreement PHY-0107417.

This paper has been assigned LIGO Document Number LIGO-P060056-00-Z.

7. References

[1] Forward, R. L. and Miller, L. R. *J. Appl. Phys.*, 38:512–+, 1967.

[2] J. Sinsky and J. Weber. New Source for Dynamical Gravitational Fields. *Physical Review Letters*, 18:795–797, May 1967.

[3] J. A. Sinsky. Generation and Detection of Dynamic Newtonian Gravitational Fields at 1660 cps. *Physical Review*, 167:1145–1151, March 1968.

[4] H. Hirakawa, K. Tsubono, and K. Oide. Dynamical test of the law of gravitation. *Nature*, 283:184–+, January 1980.

[5] K. Oide, K. Tsubono and H. Hirakawa. *Jap. J. Appl. Phys.*, 19:L123, 1980.

[6] T. Suzuki, K. Tsubono and K. Kuroda. *Jap. J. Appl. Phys.*, 20:L498, 1981.

[7] Y. Ogawa, K. Tsubono, and H. Hirakawa. Experimental test of the law of gravitation. *Phys. Rev. D.*, 26:729–734, August 1982.

[8] K. Kuroda and H. Hirakawa. Experimental test of the law of gravitation. *Phys. Rev. D.*, 32:342–346, July 1985.

[9] Astone P. et al. *Z. Phys. C*, 50:21–+, 1991.

[10] Astone P. et al. Experimental study of the dynamic Newtonian field with a cryogenic gravitational wave antenna. *European Physical Journal C*, 5:651–664, 1998.

[11] Abbott B. et al. Detector description and performance for the first coincidence observations between LIGO and GEO. *Nuclear Instruments and Methods in Physics Research A*, 517:154–179, January 2004.

[12] D. Sigg and the LIGO Science Collaboration. Status of the LIGO detectors. *Classical and Quantum Gravity*, 23:51–+, April 2006.

[13] Acernese, F. et al. *Classical and Quantum Gravity*, 23:S63, 2006.

[14] Takahashi, R. et al. *Classical and Quantum Gravity*, 21:S403, 2004.

[15] Lück, H. et al. *Classical and Quantum Gravity*, 23:S71, 2006.

[16] http://www.ligo.caltech.edu/advLIGO.

[17] P. R. Saulson. Terrestrial gravitational noise on a gravitational wave antenna. *Phys. Rev. D.*, 30:732–736, August 1984.

[18] S. A. Hughes and K. S. Thorne. Seismic gravity-gradient noise in interferometric gravitational-wave detectors. *Phys. Rev. D.*, 58(12):122002–+, December 1998.

[19] Beccaria M. et al. Relevance of Newtonian seismic noise for the VIRGO interferometer sensitivity. *Class. Quantum Grav.*, 15:3339–3362, 1998.

[20] R. Spero. Prospects for Ground Based Detectors of Low Frequency Gravitional Radiation. *AIP Conf. Proc.*, 96:347–350, 1983. in Science Underground.

[21] T. Suzuki and H. Hirakawa. Local Field and Gravitational Radiation Experiments. *J. Phys. Soc. Japan*, 48(2):685–686, 1980.

[22] L. Matone et al. Input Test Mass (ITM) Absolute Calibrations: Fringe Counting, Fringe Fitting, and Sign Toggling Methods. 2002. LIGO Internal Document T020141.

[23] R. Adhikari et al. Calibration of the LIGO detectors for the First LIGO Scientific Run. 2003. LIGO Internal Document T030097.

[24] D. Sigg. Strain Calibration in LIGO. 1997. LIGO Internal Document T970101.

[25] J. Bruursema. Calibration of the LIGO Interferometer Using the Recoil of Photons. 2003. LIGO Internal Document T030266.

[26] E. Goetz. Commissioning of the Photon Calibrators. 2004. LIGO Internal Document T040196.

[27] P. Kalmus. Commissioning of the Photon Calibrators for S5. 2005. LIGO Internal Document T050221.

[28] G. Gonzalez et al. Calibration of the LIGO detectors for S3. 2005. LIGO Internal Document T050059.

[29] P. Raffai, L. Matone, S. Marka, I. Bartos, Z. Marka. Tests of non-Newtonian Gravity Using Dynamic Gravity-Gradients in Interferometric Gravitational-Wave Detectors. *Phys. Rev. D.*, to be submitted.

[30] J. Hazel S. Kawamura and F. Raab. Suspension Preliminary Design. 1996. LIGO Internal Document T960074.

[31] LIGO collaboration. Displacement Sensitivities for the LIGO Interferometers - Early Performance for S5. 2006. LIGO Internal Document G060011.

[32] Sartorius CC10000U-L, http://sartorius.balances.com/sartorius/mass-comparators.html.

[33] in the case of Titanium, see for example http://www.cranfieldprecision.com/.

[34] E. Morganson. Developing an Earth-Tides Model for LIGO Interferometers. 1999. LIGO Internal Document T990181.

[35] L. Matone. Slow Ground Motion Observed by LIGO. 2000. LIGO Internal Document G000325.

[36] K. Minoshima and H. Matsunoto. *Conference on Lasers and Electro-Optics Europe High-precision distance measurement using the frequency comb of an ultrashort pulse laser*, page 440, 2005.

[37] personal conversation, M. Landry.

[38] J.Giaime et al. *Rev. Sci. Instr.*, 67:208, 1996.